SUGISAKA MASANORI

Journal of Advances in Artificial Life Robotics
Vol. 3(4); March (2023), pp. 242–249
ON LINE ISSN 2435-8061; ISSN-L 2435-8061
https://alife-robotics.org/jallr.html

Research Article

An Analysis of Robot Speed Efficiency for Mobile Robot Adapted Three Omni Rollers Using Linear Transformation

Kenji Kimura[1], Yuki Shigyo[2], Kazuo Ishii[3]
[1]*Department of Control Engineering, National Institute of Technology, Matsue College, 14-4 Nishi-ikuma-cho, Matsue-shi, Shimane, 690-8518, Japan*
[2]*Digital Solution Div, DX Engagement Dept, Fujitsu, 3-5-20 Minamikamata. Ota City, Tokyo 144-0035, Japan*
[3]*Graduate School of Life Science and engineering, Kyushu Institute of Technology, 2-4 Hibikino, Wakamatsu-ku, Kitakyushu-shi, 808-0196, Fukuoka, Japan*

ARTICLE INFO

Article History

Received 10 November,2022
Accepted 05 July 2023

Keywords

Omni-roller
Transformation matrix
Motion analysis of mobile robot

ABSTRACT

RoboCup Middle-sized-League soccer robots are mainly equipped with the three omni-roller mechanism. These mobile robots are expected to function efficiently in fields, such as logistics. These systems are easy to control and allow omnidirectional movement. However, theoretical research on these systems' exercise efficiencies has not been conducted. In this research, we assume a mechanism that can arbitrarily change the roller arrangement based on a circular mechanism and evaluate the roller arrangement from a speed efficiency perspective. Additionally, we define an evaluation function using the theory of linear transformation to examine the roller arrangement.

1. Introduction

RoboCup soccer robot incorporates two important elements. The first is a ball holding mechanism that dribbles the ball, and the second is a moving mechanism using three omni rollers. There are studies on ball holding mechanisms, such as RV-infinity [1], Musashi150 [2], and NuBot [3]. Studies on a sphere driven by two rollers were conducted [4], [5], as research on kinematics. Furthermore, numerous studies are focused on the kinetic energy of rollers for efficient spherical transportation [6], [7], [8], [9].

Considering omnidirectional movement, mobile robots have recently been developed in various fields, including physical distribution. Omnidirectional motion with nonholonomic or holonomic properties can produce three degrees of freedom of motion (i.e., two translational degrees of freedom and one rotational degree of freedom). Among them, the holonomic movement mechanism is easy to control as the wheels are independently driven and have excellent mobility in all directions. Using this property, a mobile robot with an equilateral triangle roller arrangement was developed [10].

Figure 1 shows three omni layout patterns of mobile robots. Particularly, many of the layout structures of Type (X), adopted in Figure 1(a), are also found in RoboCup MSL robots [1], [2], [3]. Moreover, Type (Y) and Type (Z) presented in Figures 1(b) and (c) are conceivable. However, not only the RoboCup MSL robot but also other mobile robots adopt the regular polygon arrangement, which is the most

Corresponding author's E-mail: k-kimura@matsue-ct.jp, shigyo.yuki@fujitsu.com, ishii@brain.kyutech.ac.jp

symmetrical polygon, as shown in Figure 1(a). Besides, no theoretical research has been conducted on this kinematics

In this research, we consider generalizing the conventional equilateral triangle arrangement [11]. Therefore, we derive general kinematics assuming a mechanism can arbitrarily change the position of rollers using a circular mechanism, derive a transformation matrix that associates input and output, and adopt the value of the determinant as the evaluation function. Additionally, the roller arrangement is evaluated in terms of speed efficiency. Here, "image volume" and "orthographic projection area" are adopted as evaluation functions.

The rest of this study is as follows: Chapter 2 discusses the kinematics of mobile robots and defines an evaluation function. Chapter 3 conducted the simulation. Finally, we present the summary and future tasks.

2. General mobile robot kinematics for three-omni roller

In this section, we derive kinematics (inverse and forward) in a mechanism that can change the position of rollers arbitrarily. Assuming motion on a horizontal plane, the kinematics of the robot with reference [11] are similar. Here, the focus is on the relationship between the rotational speed of the driven omni-wheel and the speed of the robot.

Table 1 shows variables list of this research. Figure 2 shows parameters for mobile robot adapted three omni-roller. Curcic shape robot which has a common radius L adapts three omni-wheels. The *k-th* rollers ($k = 1,2,3$) contact position $\boldsymbol{q_i}$ on a periphery of robot, which has a

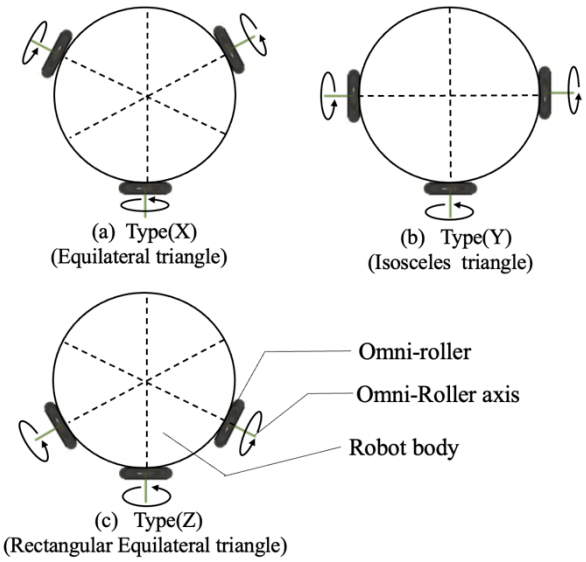

Figure 1 Example of an isosceles triangle in three rollers arrangement pattern for mobile robots.

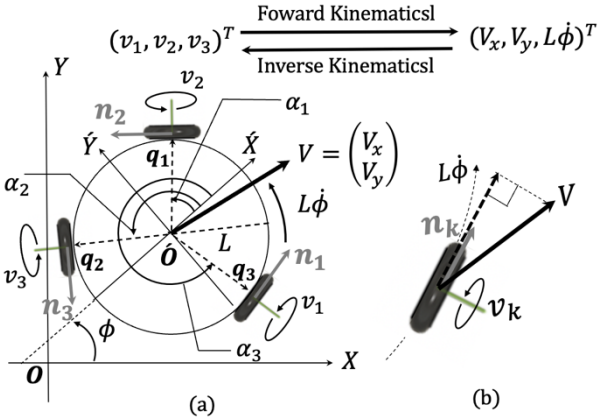

Figure 2 Parameters for mobile robot mechanism adapted three omni-roller (a) mechanism of mobile robot (b). focus on neighborhood of single roller.

roller of radius R distance between rollers and floor. $\Sigma - XY$ denotes the global coordinate. system (origin $\boldsymbol{O}$) and $\Sigma - \acute{X}\acute{Y}$ denotes robot coordinate system (origin $\acute{\boldsymbol{O}}$). The mobile robot orientation angle ϕ is defined as the angle between X-axis and $\acute{X}$-axis. $\{\boldsymbol{n_1}, \boldsymbol{n_2}, \boldsymbol{n_3}\}$ represents the unit vector along the roller velocity direction. Roller peripheral speed v_k is calculated from given $\boldsymbol{V} = (V_x, V_y)^{\boldsymbol{T}}$ and φ denotes robot direction for $\Sigma - \acute{X}\acute{Y}$ and $\dot{\phi}$ denotes robot angular velocity.

2.1. *Derive of inverse kinematics*

Table 1 Variables list of this research

$\Sigma - XY$	Two-dimensional grovel coordinate system
$\Sigma - \acute{X}\acute{Y}$	Two-dimensional robot coordinate system
$\langle \boldsymbol{a}, \boldsymbol{b} \rangle$	Inner product with respect to vector $\boldsymbol{a}$ and $\boldsymbol{b}$
$\|\boldsymbol{a}\|$	Norm of vector $\boldsymbol{a}$
$\|a\|$	Absolut value of real member a
$(\boldsymbol{a})_z$	z-component of vector $\boldsymbol{a}$
$\boldsymbol{V}$	Mobile velocity of sphere on xy-plane
$\boldsymbol{O}$	Origin of $\Sigma - xy$
$\boldsymbol{q_i}$	Rollers contact position
$\boldsymbol{\acute{O}}$	Origin of $\Sigma - \acute{X}\acute{Y}$
$\boldsymbol{n_i}$	unit vector along the velocity vector of roller
L	Radius of mechanism body
R	Radius of omni-roller
ϕ	Angle between X-axis and $\acute{X}$-axis
v_k	Roller peripheral speed
v_k^T	Translation components of v_k
v_k^R	Rotational components of v_k
α_k	Position angle of $\boldsymbol{q_k}$
$\dot{\phi}$	Robot angular velocity
W	Cubic domain that has a square, 2 $[m/s]$
f_A	Linear transformation mapping of matrix $\boldsymbol{A}$
$f_{A^{-1}}(W)$	Invers image of W
$f_{\boldsymbol{A}^{-1}}\acute{}(W)$	Orthographic projection domain of $f_{A^{-1}}(W)$
D_{Vol}	Image volume (Volume of $f_{A^{-1}}(W)$)
D_{Are}	Orthographic projection area (Area of $f_{\boldsymbol{A}^{-1}}\acute{}(W)$)
$(\boldsymbol{a_1}, \boldsymbol{a_2}, \boldsymbol{a_2})$	Vectors represent of matrix $\boldsymbol{A}^{-1}$
$\boldsymbol{\acute{a}_k}$	projection vector of $\boldsymbol{a_k}$ with respect to horizontal plane
D_V	Volume of $f_{A^{-1}}(W)$
D_A	Area of $f_{\boldsymbol{A}^{-1}}\acute{}(W)$

Robot speed are decomposed translation components v_i^T and rotational components v_k^R. Rollers contact position $\boldsymbol{q_k}$ are adapted angle α_k $(0° \leq \alpha_k < 360°)$ on the circle that has a radius of body L.

$$\boldsymbol{q_i} = L(\cos\alpha_k, \sin\alpha_k)^{\boldsymbol{T}} \tag{1}$$

From unit vector $\boldsymbol{n_k}$ is perpendicular to $\boldsymbol{q_k}$ and $\boldsymbol{n_k}$ is represented as Eq. (2).

$$\boldsymbol{n_k} = (-\sin\alpha_k, \cos\alpha_k)^{\boldsymbol{T}} \tag{2}$$

Thus. Translation component v_k^T is length of orthogonal projection vector of $\boldsymbol{V}$ with respect to $\boldsymbol{n_k}$.Thus. $v_k^T = \langle \boldsymbol{n_k}, (V_x, V_y)^{\boldsymbol{T}} \rangle$. Moreover. robot rational component v_k^R is equal to $L\dot{\phi}$. Therefore v_k is represented as the sum of the translation component and rotational component as Eq. (3).

$$v_k = v_k^T + v_k^R \tag{3}$$

$$= \langle \boldsymbol{n_k}, (V_x, V_y)^{\boldsymbol{T}} \rangle + L\dot{\phi} \tag{4}$$

Substituting Eq. (2) with Eq. (4) in each $v_k(k = 1,2,3)$, $(v_1, v_2, v_3)^{\boldsymbol{T}}$ is represented using matrix.

$$\begin{pmatrix} v_1 \\ v_2 \\ v_3 \end{pmatrix} = \begin{pmatrix} -\sin\alpha_1 & \cos\alpha_1 & 1 \\ -\sin\alpha_2 & \cos\alpha_2 & 1 \\ -\sin\alpha_3 & \cos\alpha_3 & 1 \end{pmatrix} \begin{pmatrix} V_x \\ V_y \\ L\dot{\phi} \end{pmatrix} \tag{5}$$

2.2. *Derive of forward kinematics*

Here., we put (3,3) matrix right side of Eq. (5) to $\boldsymbol{A}$. Eq. (5) is solved to $(V_x, V_y, L\dot{\phi})^T$ as follow.

$$\begin{pmatrix} V_x \\ V_y \\ L\dot{\phi} \end{pmatrix} = (\det\boldsymbol{A})^{-1} \tag{6}$$

$$\begin{pmatrix} \cos\alpha_2 - \cos\alpha_3 & -\cos\alpha_1 + \cos\alpha_3 & \cos\alpha_1 - \cos\alpha_2 \\ \sin\alpha_2 - \sin\alpha_3 & -\sin\alpha_1 + \sin\alpha_3 & \sin\alpha_1 + \sin\alpha_2 \\ -\sin(\alpha_2 - \alpha_3) & -\sin(\alpha_3 - \alpha_1) & -\sin(\alpha_1 - \theta_2) \end{pmatrix} \begin{pmatrix} v_1 \\ v_2 \\ v_3 \end{pmatrix}$$

where

$$\det\boldsymbol{A} = -\sin(\alpha_1 - \alpha_2) - \sin(\alpha_2 - \alpha_3) - \sin(\alpha_3 - \alpha_1) \tag{7}$$

(See **Appendix(A)**)

3. Evaluation function for roller arrangement

In this chapter, we make a connection $\boldsymbol{A}$ (in Eq. (5)) with the rollers contact position in mobile robot and evaluate roller arrangement using noble evaluation function such as "Image volume," "orthographic projection area".

Figure 3 shows linear transformation mapping for matrix A and correspondence two space ie. $f_{\boldsymbol{A}}$: $(V_x, V_y, \dot{\phi}L) \rightarrow (v_1, v_2, v_3)$. Now. We define W as cubic domain that has a square, 2 $[m/s]$ on each side as following.

$$W = \{(v_1, v_2, v_3) \mid |v_1|, |v_2|, |v_3| \leq 1\} \tag{8}$$

(a) Three-dimensional image domain

From inverse linear transformation mapping $f_{A^{-1}}: (v_1, v_2, v_3) \rightarrow (V_x, V_y, \dot{\phi}L)$, image of cubic domain W is equal to parallelepiped domain in three-dimensional coordinate space. Using inverse matrix of linear transformation $\boldsymbol{A}^{-1} = (\boldsymbol{a_1}, \boldsymbol{a_2}, \boldsymbol{a_3})$, Inverse image $f_{\boldsymbol{A}^{-1}}(W)$ is represented as follows.

$$f_{A^{-1}}(W) = \tag{9}$$

$$\{(V_x, V_y, L\dot{\phi}) |\, v_1\boldsymbol{a_1} + v_2\boldsymbol{a_2} + v_3\boldsymbol{a_3},\ |v_1|, |v_2|, |v_3| \le 1\}$$

where

$$\boldsymbol{a_1} = (\det\boldsymbol{A})^{-1}\begin{pmatrix}\cos\alpha_2 - \cos\alpha_3\\ \sin\alpha_2 - \sin\alpha_3\\ -\sin(\alpha_2 - \alpha_3)\end{pmatrix},$$

$$\boldsymbol{a_2} = (\det\boldsymbol{A})^{-1}\begin{pmatrix}-\cos\alpha_1 + \cos\alpha_3\\ -\sin\alpha_1 + \sin\alpha_3\\ -\sin(\alpha_3 - \alpha_1)\end{pmatrix}$$

$$\boldsymbol{a_3} = (\det\boldsymbol{A})^{-1}\begin{pmatrix}\cos\alpha_1 - \cos\alpha_2\\ \sin\alpha_1 + \sin\alpha_2\\ -\sin(\alpha_1 - \alpha_2)\end{pmatrix} \tag{10}$$

Besides, Using matrix property. $\det(\boldsymbol{A}^{-1})$ is equal to $(\det\boldsymbol{A})^{-1}$. linear transformation property is that determinant is equal to the volume ratio from two space. In this research, we define the volume of $f_{A^{-1}}(W)$ as $D_V(\alpha_1, \alpha_2, \alpha_3)$. Moreover, using $\det(\boldsymbol{A}^{-1})$, image volume is calculated as follows (See **Appendix(B)**).

$$D_V(\theta_1, \theta_2, \theta_3) = 8\,/\det\boldsymbol{A}\ [m/s]^3 \tag{11}$$

Particularly, we analyze a case that contact position triangle $\{\boldsymbol{q_1}, \boldsymbol{q_2}, \boldsymbol{q_3}\}$ represents the isosceles triangle as $\boldsymbol{q_1q_3} = \boldsymbol{q_2q_3}$. As shown in Eq. (11), $\det \boldsymbol{A}$ is three parametric function with respect to α_1, α_2 and α_3. Substituting Eq. (11) with $\alpha_1 = \theta$, $\alpha_2 = 180° - \theta$, and $\alpha_3 = 270°$, we obtain Eq. (12)

$$D_V(\theta) = \frac{8}{2\cos\theta + \sin 2\theta} \tag{12}$$

And. Theoretically, $D_V(\theta_1, \theta_2, \theta_3)$ takes minimal value when $\{\boldsymbol{q_1}, \boldsymbol{q_2}, \boldsymbol{q_3}\}$ is equilateral triangle (See **Appendix(C)**).

(b) Two-dimensional orthographic projection domain

Next, $\acute{\boldsymbol{a}}_{\boldsymbol{k}}$ is the projection vector of $\boldsymbol{a_k}$ with respect to the (V_x, V_y)-plane. Following $f_{\acute{A}^{-1}}(W)$ can be defined

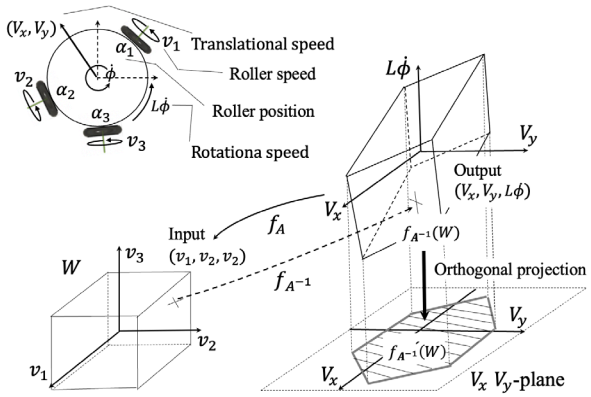

Figure 3 Linear transformation mapping correspondence between three rollers speed $\{v_1, v_2, v_3\}$ and robot (mobile speed (V_x, V_y)), and rotational speed $\dot{\phi}$.

the projection area of domain $f_{\boldsymbol{A}^{-1}}(W)$ for horizontal plane as Eq. (13).

$$f_{\acute{A}^{-1}}(W) = \tag{13}$$

$$\{(V_x, V_y) |\, v_1\acute{\boldsymbol{a}}_{\boldsymbol{1}} + v_2\acute{\boldsymbol{a}}_{\boldsymbol{2}} + v_3\acute{\boldsymbol{a}}_{\boldsymbol{3}},\ |v_1|, |v_2|, |v_3| \le 1\}$$

where

$$\acute{\boldsymbol{a}}_{\boldsymbol{1}} = (\det\boldsymbol{A})^{-1}\begin{pmatrix}\cos\alpha_2 - \cos\alpha_3\\ \sin\alpha_2 - \sin\alpha_3\\ 0\end{pmatrix}$$

$$\acute{\boldsymbol{a}}_{\boldsymbol{2}} = (\det\boldsymbol{A})^{-1}\begin{pmatrix}-\cos\alpha_1 + \cos\alpha_3\\ -\sin\alpha_1 + \sin\alpha_3\\ 0\end{pmatrix}$$

$$\acute{\boldsymbol{a}}_{\boldsymbol{3}} = (\det\boldsymbol{A})^{-1}\begin{pmatrix}\cos\alpha_1 - \cos\alpha_2\\ \sin\alpha_1 + \sin\alpha_2\\ 0\end{pmatrix} \tag{14}$$

Thus. $D_A(\alpha_1, \alpha_2, \alpha_3)$ is function depended on roller contact position $(\alpha_1, \alpha_2, \alpha_3)$ and it has two case by sign of $(\acute{\boldsymbol{a}}_{\boldsymbol{2}} \times \acute{\boldsymbol{a}}_{\boldsymbol{3}})_z(\acute{\boldsymbol{a}}_{\boldsymbol{1}} \times \acute{\boldsymbol{a}}_{\boldsymbol{3}})_z$.

$$D_A = \begin{cases} 4\|\acute{\boldsymbol{a}}_{\boldsymbol{1}} \times \acute{\boldsymbol{a}}_{\boldsymbol{2}}\| + 4\|(\acute{\boldsymbol{a}}_{\boldsymbol{1}} - \acute{\boldsymbol{a}}_{\boldsymbol{2}}) \times \acute{\boldsymbol{a}}_{\boldsymbol{3}}\| \\ \qquad [\,(\acute{\boldsymbol{a}}_{\boldsymbol{2}} \times \acute{\boldsymbol{a}}_{\boldsymbol{3}})_z(\acute{\boldsymbol{a}}_{\boldsymbol{1}} \times \acute{\boldsymbol{a}}_{\boldsymbol{3}})_z < 0] \\ 4\|\acute{\boldsymbol{a}}_{\boldsymbol{1}} \times \acute{\boldsymbol{a}}_{\boldsymbol{2}}\| + 4\|(\acute{\boldsymbol{a}}_{\boldsymbol{1}} + \acute{\boldsymbol{a}}_{\boldsymbol{2}}) \times \acute{\boldsymbol{a}}_{\boldsymbol{3}}\| \\ \qquad [\,(\acute{\boldsymbol{a}}_{\boldsymbol{2}} \times \acute{\boldsymbol{a}}_{\boldsymbol{3}})_z(\acute{\boldsymbol{a}}_{\boldsymbol{1}} \times \acute{\boldsymbol{a}}_{\boldsymbol{3}})_z > 0] \end{cases} \tag{15}$$

(See **Appendix(D)**)

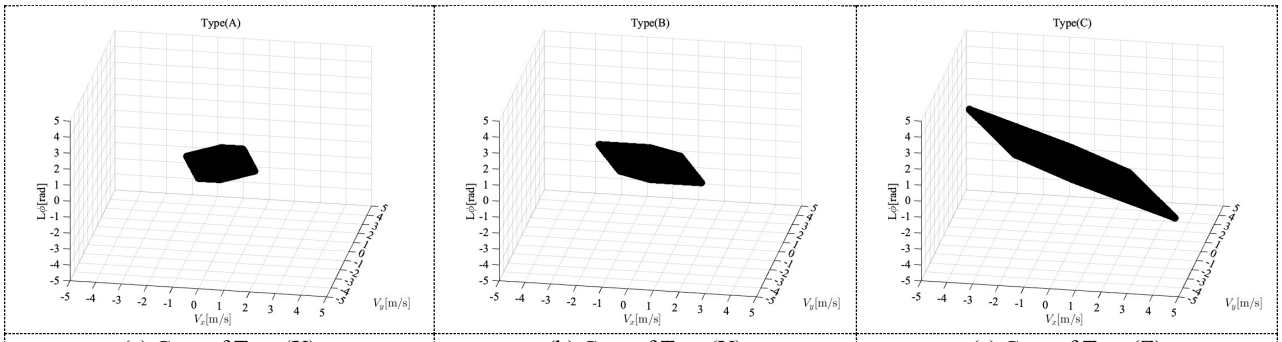

(a) Case of Type(X) (b) Case of Type(Y) (c) Case of Type(Z)

Figure 4 Three-dimensional shape of inverse image of W

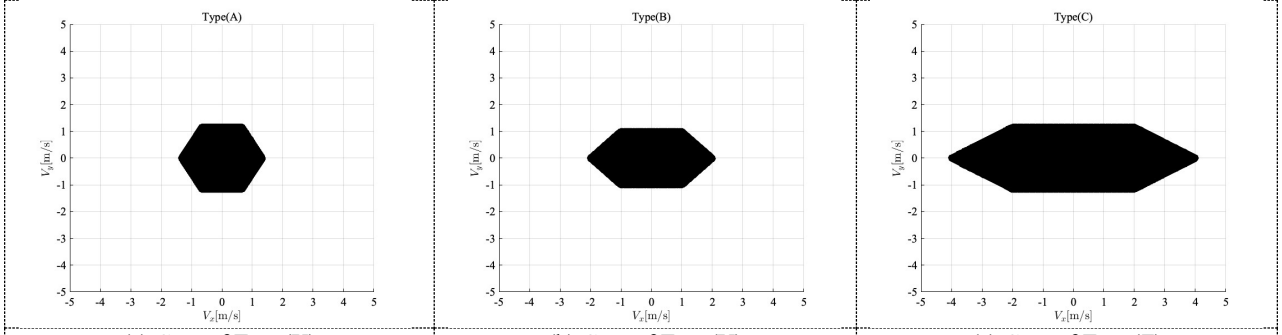

(a) Case of Type(X) (b) Case of Type(Y) (c) Case of Type(Z)

Figure 5 Two-dimensional shape of $f_{A^{-1}}(W)$

4. Simulation

This section presents the simulation findings (behavior and shape), including the evaluation values as image volume and orthographic projection area .

Simulations were performed at the three various roller arrangement Type(X)-(Z) that $\boldsymbol{q_1}$, $\boldsymbol{q_2}$, and $\boldsymbol{q_3}$ are arranged a symmetry triangle shaped (See Figure1).
They are set up α_k $(k = 1,2,3)$ as follows:
Type(X): $\{\alpha_1, \alpha_2, \alpha_3\} = \{30°, 150°, 270°\}$
Type(Y): $\{\alpha_1, \alpha_2, \alpha_3\} = \{0°, 180°, 270°\}$
Type(Z): $\{\alpha_1, \alpha_2, \alpha_3\} = \{210°, 270°, 300°\}$
and $L = 1$[m].

Table 2 Comparison of three roller arrangement patten by the evaluation values $D_V(\theta)$ and $D_A(\theta)$

	$D_V(\theta)$ $[m/s]^3$	$D_A(\theta)$ $[m/s]^2$
Type (X)	3.08	4.61
Type (Y)	4.00	6.00
Type (Z)	9.24	13.85

Figures 4 and 5 and show the shape $f_{A^{-1}}(W)$ of Eq.(9) and $f_{A^{-1}}(W)$ of Eq.(13), respectively. for Type(X), Type(Y), and Type(Z). Table 2 shows value $D_V(\theta)$ of Eq.(12) and $D_A(\theta)$ of Eq. (15) in Type(X)–(Z). And Figure 6 shows behavior of $D_V(\theta)$ and $D_A(\theta)$ with respect to parameter θ.

As shown in Figure 4, Shape of $f_{A^{-1}}(W)$ is a parallelepiped, which is getting stretched with respect to directions V_x-axis and $L\dot{\phi}$-axis.

As shown in Figure 5, Shape of $f_{A^{-1}}(W)$ is hexagons, which is getting stretched with respect to V_x -axis direction.

As shown in Table 2, Type (X) has the smallest value $D_V(\theta)$. Additionally, since Type(Z) is the largest value of $D_V(\theta)$, the moving volume in translational motion is effective. And similar results were obtained for the evaluation $D_A(\theta)$.

As shown in Figure 6, $D_V(\theta)$ and $D_V(\theta)$ take minimal values when $\theta = 30°$.

In this way, we geometrically obtain the distribution and property of $f_{A^{-1}}(W)$ and $f_{A^{-1}}(W)$. Furthermore, we get property of image volume $D_V(\theta)$ and orthographic projection area $D_A(\theta)$ and we clear that effective and ineffective roller arrangement.

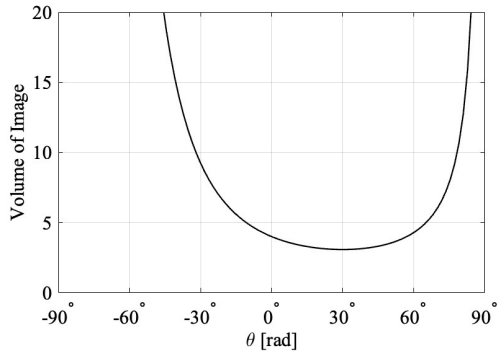

(a)

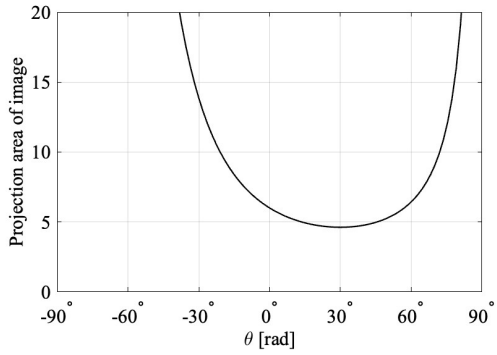

(b)

Figure 6 Behavior of evaluation functions with respect to parameter θ (a). Case of $D_V(\theta)$ $[m/s]^3$ (b). Case of D_A $(\theta)[m/s]^2$

4. Conclusions

In this research, we derived kinematics for a mobile robot that adapted three omni rollers that can arbitrarily change the roller arrangement position. Additionally, we adopted the determinant of the transformation matrix that associates the input and output as an evaluation function to examine the roller arrangement.

The following results were obtained: the evaluation function was minimized in an equilateral triangle arrangement (Type(X)). Furthermore, Type(Z) is the most efficient considering the translational motion. Therefore, motion evaluation of a translational mechanism is the only future challenge in this field.

As futures works, we'll conducted experiment using prototype adapted three omni roller.

Appendix

(A) Calculation of inverse matrix

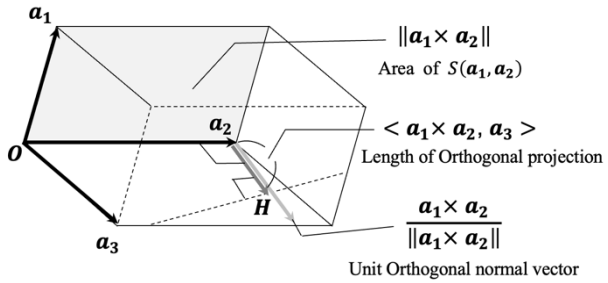

Figure 7 Calculation of volume of parallelepiped domain

Substitute the cofactor of $a_{i,j}$ with $\widetilde{a_{i,J}}$, We obtain the following using the cofactor.

$$\boldsymbol{A}^{-1} = \frac{1}{\det\boldsymbol{A}}\begin{bmatrix}\widetilde{a_{1,1}} & \widetilde{a_{1,2}} & \widetilde{a_{1,3}}\\ \widetilde{a_{2,1}} & \widetilde{a_{2,2}} & \widetilde{a_{2,3}}\\ \widetilde{a_{3,1}} & \widetilde{a_{3,2}} & \widetilde{a_{3,3}}\end{bmatrix} \tag{A,1}$$

where

$$\begin{aligned}\widetilde{a_{1,1}} &= L\cos\alpha_2 - L\cos\alpha_3\\ \widetilde{a_{2,2}} &= -L\sin\alpha_1 + L\sin\alpha_1\\ \widetilde{a_{1,2}} &= -L\cos\alpha_1 + L\cos\alpha_3\\ \widetilde{a_{2,1}} &= L\sin\alpha_2 - L\sin\alpha_3\\ \widetilde{a_{1,3}} &= L\cos\alpha_1 - L\cos\theta_1\\ \widetilde{a_{2,3}} &= L\sin\alpha_1 - L\sin\alpha_2\end{aligned} \tag{A,2}$$

And

$$\det\boldsymbol{A} = \widetilde{a_{3,1}} + \widetilde{a_{3,2}} + \widetilde{a_{3,3}} \tag{A,3}$$

where

$$\begin{aligned}\widetilde{a_{3,1}} &= -\sin\alpha_2\cos\alpha_3 + \cos\alpha_2\sin\alpha_3\\ &= -\sin(\alpha_2-\alpha_3)\\ \widetilde{a_{3,2}} &= \sin\alpha_1\cos\alpha_3 - \cos\alpha_1\sin\alpha_3\\ &= \sin(\alpha_1-\alpha_3)\\ \widetilde{a_{3,3}} &= -\sin\alpha_1\cos\alpha_2 + \cos\alpha_1\sin\alpha_2\\ &= \sin(\alpha_2-\alpha_1)\end{aligned} \tag{A,4}$$

(B) Calculation of image volume

As shown in Figure 7, The parallelepiped domain is spanned by $\{\boldsymbol{a_1},\boldsymbol{a_2},\boldsymbol{a_3}\}$. Upward plane spanned by $\{\boldsymbol{a_1},\boldsymbol{a_2}\}$ have area $\|\boldsymbol{a_1}\times\boldsymbol{a_2}\|$ and unit normal vector $\boldsymbol{a_1}\times\boldsymbol{a_2}/\|\boldsymbol{a_1}\times\boldsymbol{a_2}\|$.

Length of orthographic projection vector $\overrightarrow{\mathbf{OH}}$ is represented as follows.

$$\mathbf{OH} = \frac{1}{\|\boldsymbol{a_1}\times\boldsymbol{a_2}\|}\langle\boldsymbol{a_1}\times\boldsymbol{a_2},\boldsymbol{a_3}\rangle \tag{B,2}$$

Therefore. volume is calculated as follows.

$$\boldsymbol{V} = \|\boldsymbol{a_1} \times \boldsymbol{a_2}\| \times \overline{\mathbf{OH}} \tag{B,3}$$

Moreover, using determinant property,

$$\boldsymbol{V} = \langle \boldsymbol{a_1} \times \boldsymbol{a_2}, \boldsymbol{a_3} \rangle = \det[\boldsymbol{a_1}, \boldsymbol{a_2}, \boldsymbol{a_3}] \tag{B,3}$$

*(C) **Minimalize of function in Type(X)***

Now, we conduct a change of variables $(\alpha_1, \alpha_2, \alpha_3) \rightarrow (A, B, C)$ as follows:

$$\alpha_2 - \alpha_1 = A,\ \alpha_3 - \alpha_2 = B,\ \ C = 360° - A - B \tag{C,4}$$

$\sin(\theta_1 - \theta_3)$. We can simplify using $\theta_3 - \theta_1 = A + B = 360° - C$ as follows:

$$\sin(\alpha_1 - \alpha_3) = \sin(C - 360°) = \sin C \tag{C,5}$$

Thus, Eq. (A,3) is denoted by a simple equation.

$$\det\boldsymbol{A} = L(\sin A + \sin B + \sin C) \quad (A + B + C = 360°) \tag{C,6}$$

$\sin t$ is an upward convex function with respect to t and it takes a maximal value when $t = (A + B + C)/3 = 120°$. Thus, $1/\det\boldsymbol{A}$ has maximal value. we find out that $D_V(\theta)$ was minimized in the equilateral triangle arrangement (i.e., Type(X)).

***(D) Calculation of** D_A*

Using column vector $\boldsymbol{\acute{a}_k}$, $[V_x, V_y]^{\boldsymbol{T}}$ is denoted by a linear combination of $\boldsymbol{\acute{a}_1}$, $\boldsymbol{\acute{a}_2}$ and $\boldsymbol{\acute{a}_3}$ as follow.

$\boldsymbol{U}$ denote district set as $v_3 = 0$ from $f_{\boldsymbol{A}^{-1}}(W)$ as follows.

$$\boldsymbol{U} = \{v_1\boldsymbol{\acute{A}_1} + v_2\boldsymbol{\acute{A}_2} \,|\, |v_1|, |v_2| \le 1\} \tag{D,1}$$

We consider that shape when U move on a line trajectory of direction $\boldsymbol{\acute{a}_3}$(as parameter v_3) as follows. Figure 8(a) shows two cases proving the following **Case 1** and **Case 2** of a layout condition of $\{\boldsymbol{\acute{a}_1}, \boldsymbol{\acute{a}_2}, \boldsymbol{\acute{a}_3}\}$ with a focus on the direction $\boldsymbol{\acute{a}_3}$.

Case 1: $\boldsymbol{\acute{a}_3}$ is lay from $\boldsymbol{\acute{a}_1}$ and $\boldsymbol{\acute{a}_2}$, or $\boldsymbol{\acute{a}_3}$ is lay from $-\boldsymbol{\acute{a}_1}$ and $-\boldsymbol{\acute{a}_2}$.

This condition is derived as follows.

$$\{(\boldsymbol{\acute{a}_2} \times \boldsymbol{\acute{a}_3})_z < 0 \text{ and } (\boldsymbol{\acute{a}_1} \times \boldsymbol{\acute{a}_3})_z > 0\}$$

$$\text{or } \{(\boldsymbol{\acute{a}_2} \times \boldsymbol{\acute{a}_3})_z > 0 \text{ and } (\boldsymbol{\acute{a}_1} \times \boldsymbol{\acute{a}_3})_z < 0\} \tag{D,2}$$

$$\Leftrightarrow \quad (\boldsymbol{\acute{a}_2} \times \boldsymbol{\acute{a}_3})_z (\boldsymbol{\acute{a}_1} \times \boldsymbol{\acute{a}_3})_z < 0] \tag{D,3}$$

Figure 8(b) shows when v_3 is vanished or fixed, $\boldsymbol{U}$ will be a parallelogram. Thus, the trajectory trac of $\boldsymbol{U}$ in existing hexagonal domains on opposite sides are parallel. Thus, Half of the domain is the sum of the area of $\square \boldsymbol{R_+P_+PR}$ and $\triangle \boldsymbol{Q_+P_+R_+}$. Hence, D_A is represented as Eq. (12).

Case 2: $\boldsymbol{\acute{a}_3}$ is lay from $\boldsymbol{\acute{a}_1}$ and $-\boldsymbol{\acute{a}_2}$. or $\boldsymbol{\acute{a}_3}$ is lay from $-\boldsymbol{\acute{a}_1}$ and $\boldsymbol{\acute{a}_2}$.

In this case, we prove this as **Case 1,** and. D_A is represented as Eq. (12).

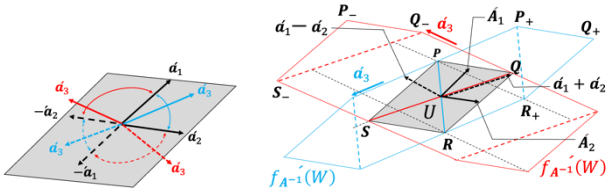

Figure 8 (a) Layout condition of $\{\boldsymbol{\acute{a}_1}, \boldsymbol{\acute{a}_2}, \boldsymbol{\acute{a}_3}\}$ focus on direction $\boldsymbol{\acute{a}_3}$. (b). Line trajectory of direction $\boldsymbol{\acute{a}_3}$ of existing hexagonal domains

References

[1] Y.Yasohara, K.Shimizu et al., Development of ball handling mechanism for RoboCup MSL, *30th Fussy System Symposium*, pp. 616-617, 2014.

[2] S. Chikushi, M. Kuwada, et al., Development of Next-Generation Soccer Robot"Musashi150"for RoboCup MSL,*30th Fussy System Symposium*, pp. 624-627,2014.

[3] R. Junkai, X. Chenggang, X. Junhao et al., A control system for active ball handling in the RoboCup middle size League, *Chinese Control and Decision Conference(CCDC.)2016.*

[4] K. Kimura, K. Ogata, K. Ishii, Novel Mathematical Modeling and Motion Analysis of a Sphere Considering Slipping, Journal of Robotics, Networking and Artificial Life, Vol.6, issue 1, pp. 27- 32, 2019.

[5] K. Kimura, S. Chikushi, K. Ishii, Evaluation of the Roller Arrangements for the Ball-Dribbling Mechanisms adopted by RoboCup Teams, Journal of Robotics, Nrtworking and Artificial Life, Vol.6, issue 3, pp. 183- 190, 2019.

[6] S. Chikushi, T.Weerakoon, T.Sonoda, K. Ishii,Journal of Robotics, Networking and Artificial Life, Vol. 4, No. 3,248–253,2017.

[7] K. Kimura, K. Ishii, Efficiency Problem of Spherical Robot in Transfer Kinetic Energy, Journal of Robotics, Networking and Artificial Life, Vol.9, issue 1, pp.87-92, 2022.

[8] K.Kimura, K.Ishii , Roller's Kinetic Energy Efficency Problem on Upper Hemisphere , 2022 Joint 12th International Conference on Soft Computing and Intelligent Systems and 23rd International Symposium on Advanced Intelligent Systems (SCIS&ISIS)2022.

[9] K.Kimura, Y.Abematsu, H.Hirai, K.Ishii, Evaluation of Two Roller Arrangement on a Hemisphere by Kinetic Energy, Journal of Robotics, Networking and Artificial Life, Vol.9, issue 3, pp.233-239, 2022.

[10] K. Kimura, K. Ishii, The Spherical Robot Transfer Problem With Minimal Total Kinetic Energy, Proceedings of International Conference on Artificial ALife and Robotics (ICAROB2021), pp.266-270, 2021.

[11] J.Tang, K.Watanabe, et al., Autonomous control for an omnidirectional mobile robot with the orthogonal-wheel

assembly, Journal of the Robotics Society of Japan. Vol. 17, No. 1,pp. 51-60, 1999.

Authors Introduction

Dr. Kenji Kimura

He is a Lecturer in the Department of Control Engineering, National Institute of Technology, Matsue College, where he has been since 2022. He received his ME (mathematics) from Kyushu University in 2002 and received his Ph.D(Engineering) from Kyushu Institute of in 2020. His research interests are spherical mobile robots.

Mr. Yuki Shigyo

He is an engineer working for Fujitsu Ltd. He received the BE from Tokyo University of Science in 2016 and the ME (mathematics) from Nagoya University in 2018. His research interests are spherical mobile robot kinematics and machine learning.

Dr. Kazuo Ishii

He is a Professor at the Kyushu Institute of Technology, where he has been since 1996. He received his Ph.D. degree in engineering from the University of Tokyo, in 1996. His research interests span both ship marine engineering and Intelligent Mechanics. He holds five patents derived from his research.